Electric Power Systems Research 235 (2024) 110846

Contents lists available at ScienceDirect

Electric Power Systems Research

journal homepage: www.elsevier.com/locate/epsr

An online cooperative control strategy for enhancing microgrid participation into electricity market

A. Cagnano [a], E. De Tuglie [b,*], A. Introna [b], P. Montegiglio [b], A. Passarelli [b]

[a] Dipartimento di Ingegneria dell'Informazione, delle Infrastrutture e dell'Energia Sostenibile, Università Mediterranea di Reggio Calabria, 89124 Reggio Calabria, Italy
[b] Dipartimento di Ingegneria Elettrica e dell'Informazione, Politecnico di Bari, 70125 Bari, Italy

ARTICLE INFO

Keywords:
Microgrids
Real-time energy management
Online economic dispatch
Multi-objective optimization problem
Lyapunov theorem

ABSTRACT

This paper develops a cooperative control methodology for the online energy management of grid-connected microgrids. The main aim of this methodology is to actively manage the active power outputs of all dispatchable energy sources available within the microgrid as well as the power exchanged with the utility grid so as to match the total load demand at the minimum operating cost. This implies to solve a constrained multi-objective dynamic optimization problem aimed at minimizing the total microgrid operating costs and ensuring the real-time balance within the microgrid in compliance with its technical-operational constraints. Lyapunov's theorem using sensitivity theory is adopted to solve this optimization.

To test the performances of the proposed control methodology, several computer simulations corresponding to different operating scenarios have been conducted on the PrInCE Lab experimental microgrid built at the Polytechnic University of Bari.

1. Introduction

Over the last decades, electric power distribution systems have undergone significant changes due to the growing integration of DERs, especially those based on renewable energy [1–4]. These changes not only covered the management and operation practices of distribution networks, but also energy market models to enable DER owners to access in the electricity markets [5]. This possibility, however, often remains unexploited due to the small capacity of such resources which may reduce their market power, thus making them individually unable to affect the energy market [6,7]. As consequence, the expected revenues of DER owners may be reduced if some remedial measures are not taken into account. In this regard, a chance can be offered by MGs since they are able to aggregate and manage DERs along with ESSs and loads so as to form a self-sufficient energy system that can operate in island or act on the main grid as a single controllable entity [8–12]. Thanks to these peculiarities, these systems can make feasible the participation of DER units to local electricity markets wherein the MG operator is responsible for coordinating local units to reduce costs and at the same time increase self-consumption within the MG.

Nonetheless, it is worth noting that their unpredictable behavior, mainly due to the intermittent outputs of their internal N-DRGs and variability of loads, can entail for MG operators the risk of paying penalties for violating power delivery agreements, resulting in the loss of a large share of revenues [13,14]. To address this issue, numerous research studies have been conducted on this topic, resulting in a variety of control solutions. Control strategies that use data-driven uncertainty modeling techniques to solve economic dispatch problems are often the focus [15–19]. Although a more efficient scheduling of MG energy resources can be obtained with these control strategies, they suffer the huge drawback of not being able to adjust the scheduled generation levels in response to unpredicted fluctuations in loads and N-DRG. As a result, the main grid acting as the One-Machine Infinite-Bus for the MG will be called to promptly compensate these internal power imbalances, giving rise to price volatility.

To overcome this issue, several studies have suggested the adoption of ESSs. Some of these references have investigated the optimal sizing of these devices [20–22], while others have focused on their optimal scheduling to maximize their daily use [23–29]. Particularly, these latter papers suggest to directly incorporate the costs associated with ESSs into the objective function of the economic dispatch problem, in order to coordinate them with other energy sources available into a MG. Depending on the considered cost for ESSs, different objective functions have been derived and optimized through several optimization algorithms. Among them, the Mixed Integer Linear Programming Method

* Corresponding author at: via Re David, 200, 70125 Bari, Italy.
E-mail address: enricoelio.detuglie@poliba.it (E. De Tuglie).

https://doi.org/10.1016/j.epsr.2024.110846
Received 25 March 2024; Received in revised form 15 May 2024; Accepted 24 June 2024
Available online 19 July 2024

Nomenclature

DER	Distributed Energy Resource.
MG	MicroGrid.
DG	Dispatchable Generator.
$N-DRG$	Non-Dispatchable Renewable Generator.
ESS	Energy Storage System.
CHP	Combined Heat and Power system.
MT	MicroTurbine.
PV	PhotoVoltaic system.
$BESS$	Battery Energy Storage System.
n	Normalization subscript index.
n_{DG}	Number of Dispatchable Generator.
n_{N-DRG}	Number of Non-Dispatchable Renewable Generator.
n_{ESS}	Number of Energy Storage System.
n_L	Number of Loads.
i	Dispatchable Generator index.
j	Non-Dispatchable Renewable Generator index.
h	Energy Storage System index.
k	Load index.
P_{TL}	Active power exchanged with the utility grid.
P_{DG}	Active power generated by Dispatchable Generators.
P_{DG}^{meas}	Active power measured at Dispatchable Generators's output.
P_{CHP}	Active power generated by Combined Heat and Power system.
P_{MT}	Active power generated by MicroTurbine.
P_{N-DRG}	Active power supplied by Non-Dispatchable Renewable Generator.
P_{PV}	Active power supplied by PhotoVoltaic system.
P_{ESS}	Active power of Energy Storage System.
P_{BESS}	Active power of Battery Energy Storage System.
P_L	Load power demand.
P_{TL}^{min}	Minimum active power exchangeable with the utility grid.
P_{TL}^{max}	Maximum active power exchangeable with the utility grid.
P_{DG}^{min}	Dispatchable Generator minimum active power limit.
P_{DG}^{max}	Dispatchable Generator maximum active power limit.

[23], the Non-Linear Programming Method [24], the Genetic Algorithm [25], stochastic models [26,27], the Teaching Learning-Based Optimization (TLBO) algorithm [28], and the Enhanced Mixed Integer Particle Swarm Optimization algorithm [29] have been demonstrated to be more effective in solving economic dispatching problems involving multiple control variables. Anyway, as outlined in [30], the performance of the aforementioned control methodologies still depends on the accuracy of the adopted forecasting methods. In the attempt to reduce the dependence on short-term forecasts, a coordinated control approach based on a two-stage optimization problem is proposed by the authors in [30]. In this paper, it is proposed a methodology that employs the classical Lagrangian approach to regulate the active power outputs of all DGs in the MG in response to real-time measurements. This adjustment is aimed to cover any active power imbalances that may occur within the MG with minimal operating costs to ensure that the actual interchange power matches the contracted value in the day-ahead energy market. It is worth noting that the performance of this methodology inevitably depends on the reliability of the communication. It is in fact necessary to receive a large amount of information in a short time to prevent that the active power exchanged with the main grid deviates from its scheduled value. Therefore, if the communication system is not fast enough, a transient active power imbalance may inevitably occur within the MG, which will be compensated by the main grid. As the compensation of these internal MG active power fluctuations is not free of charge, the net economic advantages of a MG may be reduced [31]. To overcome this issue, adaptive real-time energy management strategies have been developed in [31–33]. Most of these papers suggest compensating in the real-time the tie-line active power flow fluctuations by taking advantage of fast response times and control flexibility of ESSs. Alternatively, in [34] a real-time economic dispatching methodology employing a PI-regulator has been developed to enable MG to keep at zero the active power flow on the tie-line. The major drawback of all these methods is that they do not take into account the coordination with intraday electricity markets and thus the economic benefits of the MG may be negatively affected.

To overcome this issue, a cooperative control methodology has been developed in this paper to coordinate the local dispatching of MG-internal units with the intraday electricity market. This methodology aims to minimize MG operating costs by managing, in the online environment, the active power outputs of all its internal DGs as well as the active power exchanged with the utility grid. This entails solving a constrained multi-objective dynamic optimization problem whose objective function aims to minimize not only the production costs of DGs but also the cost of purchasing energy from the main grid, while ensuring the real-time microgrid energy balance and respecting its technical-operational constraints. An optimization algorithm based on the Lyapunov's theorem encompassing the sensitivity theory has been used to solve this optimization problem.

In order to investigate the performance of the proposed control methodology, simulations have been carried out under different operating scenarios on the PrInCE Lab experimental MG built at the Polytechnic University of Bari (Italy).

2. Mathematical formulation of the cooperative control methodology

The aim of this section is to provide the mathematical formulation of the proposed cooperative control methodology for the online energy management of a grid-connected MG. The overall optimization problem can be formulated by defining its basic elements as follows.

2.1. Control variables of the optimization problem

In this study, control variables include the active power exchanged with the utility grid and the active power outputs of all DGs available within the MG.

ESSs may also be used as control variables but, in order to extend their usage over the whole day, they were not involved in the regulation service as suggested in [30,34]. Therefore, their active power set-points were kept at the levels scheduled by the day-ahead economic dispatch as follows:

$$\boldsymbol{P}_{ESS}(t) = \overline{\boldsymbol{P}}_{ESS}(t) \tag{1}$$

where $\overline{\boldsymbol{P}}_{ESS}(t)$ are the $n_{ESS}-$ dimensional column vectors whose elements are the active power outputs of ESSs scheduled in day-ahead electricity market.

Under the above assumptions, the $(1 + n_{DG})-$ dimensional column vector of the control variables can be defined as follows:

$$\boldsymbol{x}(t) = [P_{TL}(t) \quad \boldsymbol{P}_{DG}(t)]^T \tag{2}$$

2.2. The objective function of the optimization problem

The proposed optimization problem is aimed at minimizing the total operating costs of a MG by determining the optimal trade-off between the internal active production and the active power exchanged with the utility grid in compliance with the technical-operational constraints of the system. To comply with this requirement, a multi-objective optimization problem has been formulated considering three different objective functions which will be detailed in the following subsections.

2.2.1. MG operating cost error function

The aim of this cost function is to minimize the total operating costs of the MG as much as possible. To this aim, the following scalar control error has been defined:

$$e_{MG_{Cost}}(t) \; = C_{TL}(P_{TL}(t)) + \sum_{i=1}^{n_{DG}} C_{DG_i}\left(P_{DG_i}(t)\right) \tag{3}$$

where $C_{TL}(P_{TL}(t))$ is the cost function relating to the active power exchanged with the utility grid and $C_{DG_i}(P_{DG_i}(t))$ is the cost function of the i-th DG unit.

The $C_{TL}(P_{TL}(t))$ is defined as follows:

$$C_{TL}(P_{TL}(t)) = \beta_{TL} \cdot P_{TL}(t) \tag{4}$$

where β_{TL} (€/kWh) is the cost coefficient that includes both the hourly market energy price and the distribution network charges.

In accordance with [35], the cost function related to each DG unit is instead expressed as follows:

$$C_{DG_i}\left(P_{DG_i}(t)\right) = \alpha_{DG_i} \cdot P_{DG_i}^2(t) \; + \; \beta_{DG_i} \cdot P_{DG_i}(t) + \gamma_{DG_i} \tag{5}$$

where α_{DG_i} (€/kW^{2}h), β_{DG_i} (€/kWh) and γ_{DG_i} (€/h) are the cost coefficients of the i-th DG.

2.2.2. MG active power balance error function

In order to ensure the internal MG active power balance, the following scalar error function has been considered:

$$e_{P_B}(t) \; = P_{TL}(t) + \sum_{i=1}^{n_{DG}} P_{DG_i}(t) + \sum_{j=1}^{n_{N-DRG}} P_{N-DRG_j}(t) + \sum_{h=1}^{n_{ESS}} P_{ESS_h}(t) - \sum_{k=1}^{n_L} P_{L_k}(t) \tag{6}$$

2.2.3. Error function of the active power provided by DGs

Unexpected failures of DGs could prevent them from supplying the active power required by the regulation service, moving thus the MG in a non-optimal operating condition. To make the controller capable of dealing with the unavailability of one or more DGs to provide the regulation service, the following error function has been defined:

$$\boldsymbol{e}_{P_{DG}}(t) = \mathscr{F}\left(\boldsymbol{P}_{DG}(t) - \; \boldsymbol{P}_{DG}^{meas}(t)\right) \tag{7}$$

where:

- $\mathscr{F}$ is the $n_{DG}-$ dimensional column vector of the flag parameters whose coefficients are able to enable and disable each element of the control error vector $\boldsymbol{e}_{P_{DG}}(t)$.Specifically, each element of $\boldsymbol{e}_{P_{DG}}(t)$ is disabled when its flag parameter is False (0), and initially, all flag parameters are False by default and thus $\boldsymbol{e}_{P_{DG}}(t)$ keeps silent. In case of one or more generators are unable to provide the active power required by the regulation service due to a failure, their flag parameters are turned to True (1), enabling thus the corresponding control errors to run in the control chain. These variables turn back to False when the corresponding control errors are equal to zero.

2.2.4. The multi-objective function

In order to concurrently minimize the three conflicting objectives defined in the above sections, they are normalized and merged into a single objective function given by their weighted sum, as follows:

$$\min_{\boldsymbol{x}(t)} \mathscr{L}(\boldsymbol{x}(t)) = \min_{\boldsymbol{x}(t)} \left(\frac{1}{2} \boldsymbol{e}(\boldsymbol{x}(t))^T \boldsymbol{W} \boldsymbol{e}(\boldsymbol{x}(t)) \right) \tag{8}$$

where:

- $\boldsymbol{e}(\boldsymbol{x}(t))$ is the $(1 + 1 + n_{DG})-$ dimensional column vector of the control error involving the three considered normalized objective functions as follows:

$$\boldsymbol{e}(\boldsymbol{x}(t)) = \begin{bmatrix} e_{MG_{Cost}}(\boldsymbol{x}(t))_n \\ e_{P_B}(\boldsymbol{x}(t))_n \\ \boldsymbol{e}_{P_{DG}}(\boldsymbol{x}(t))_n \end{bmatrix} \tag{9}$$

- $\boldsymbol{W}$ is a $[(1 + 1 + n_{DG}) \times (1 + 1 + n_{DG})]-$ dimensional diagonal matrix whose elements are always positive real values that weight the individual components of the control error with respect to the objective.

2.3. MG technical constraints of the optimization problem

To avoid that during the optimization process DGs are called to provide active powers exceeding their allowable constrains, their capability curve limits need to be considered as follows:

$$\boldsymbol{P}_{DG}^{\min} \leq \; \boldsymbol{P}_{DG}(t) \leq \boldsymbol{P}_{DG}^{\max} \tag{10}$$

It was also necessary to include the following operating limits on the tie-line so as to prevent the power exchanged with the utility grid can exceed the maximum available transmission capacity:

$$P_{TL}^{min} \leq \; P_{TL}(t) \leq P_{TL}^{max} \tag{11}$$

2.4. The online optimization algorithm

The main idea of the proposed methodology is to adjust the control variables, $\boldsymbol{x}(t)$, in the continuous time domain until to find the best match between the MG's internal energy production and the active power exchanged with the utility grid that minimizes the objective function stated in Eq. (8). To achieve this condition the online optimization algorithm developed in [36] has been adopted. According to this algorithm, the convergence to the minimum of the optimization problem can be ensured if the stability criteria of the Lyapunov's theorem are satisfied. For this reason, the always positive objective function $\mathscr{L}(\boldsymbol{x}(t))$ is assumed as the Lyapunov function and its time derivative is made semi-definite negative by assuming the following fictitious dynamic system:

$$\dot{\boldsymbol{x}}(t) = -k \left(\frac{\partial \mathscr{L}(\boldsymbol{x}(t))}{\partial \boldsymbol{x}(t)} \right)^T = -k \left(\frac{\partial \boldsymbol{e}(\boldsymbol{x}(t))}{\partial \boldsymbol{x}(t)} \right)^T \boldsymbol{W}^T \boldsymbol{e}(\boldsymbol{x}(t)) \tag{12}$$

where $k \in \Re^+$.

The optimal control laws $\boldsymbol{x}(t)$ can be obtained by integrating in the time domain Eq. (12):

$$\boldsymbol{x}(t) = -k \int \left(\frac{\partial \boldsymbol{e}(\boldsymbol{x}(t))}{\partial \boldsymbol{x}(t)} \right)^T \boldsymbol{W}^T \boldsymbol{e}(\boldsymbol{x}(t)) dt \tag{13}$$

Fig. 1 shows the flow-chart for the practical implementation of the proposed methodology. For clarity purposes, in this figure are also reported the interactions between the flow-chart and the physical signals coming from the MG.

Note that the proposed methodology obtains from the upper control level the hourly energy market price along with distribution network charges, cost coefficients of all DGs, as well as the active power set points of ESSs evaluated by a day-ahead economic dispatch algorithm. Based on these data and the real-time measurements of the active powers at N-

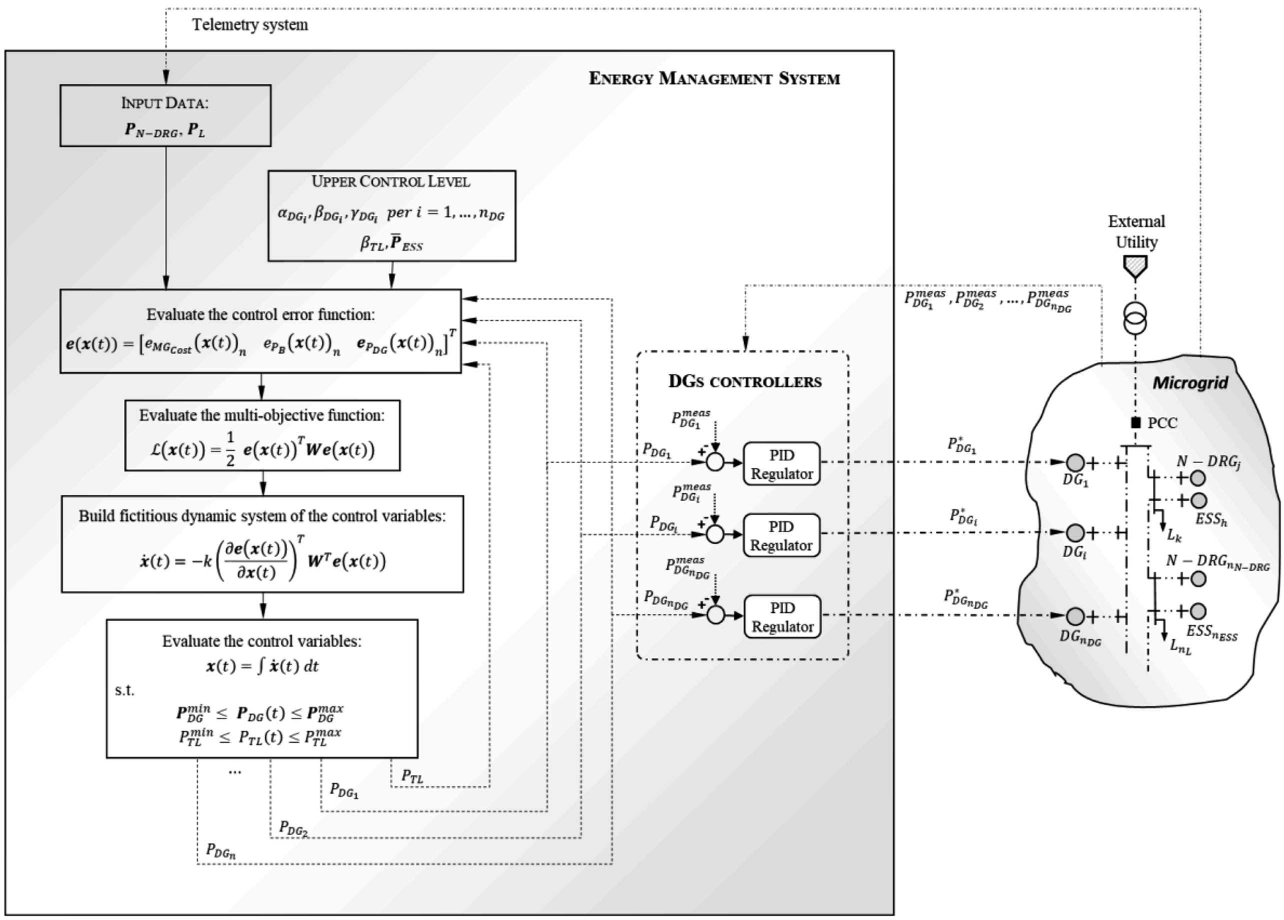

Fig. 1. Dynamic optimization controller architecture.

DRGs and load nodes, the control error $e(x(t))$ is evaluated. The resulting signal acts as input of the online optimization algorithm based on the Lyapunov theorem applied to the sensitivity theory, giving rise to the optimal control laws for DGs. To force these control actions to stay within operating limits of both the tie-line and the DGs, saturation blocks have been added.

It is noteworthy that due to their internal dynamics, DG units may provide an active power lower than that required by the regulation service moving the MG in a suboptimal operating condition. To avoid this event, DGs' controllers are included in the control loop. These controllers compare the real-time measurements of active power at DG nodes coming from the telemetry system to their reference value evaluated by the online optimization algorithm. The resulting active power error is then processed by a PID regulator providing the control laws to

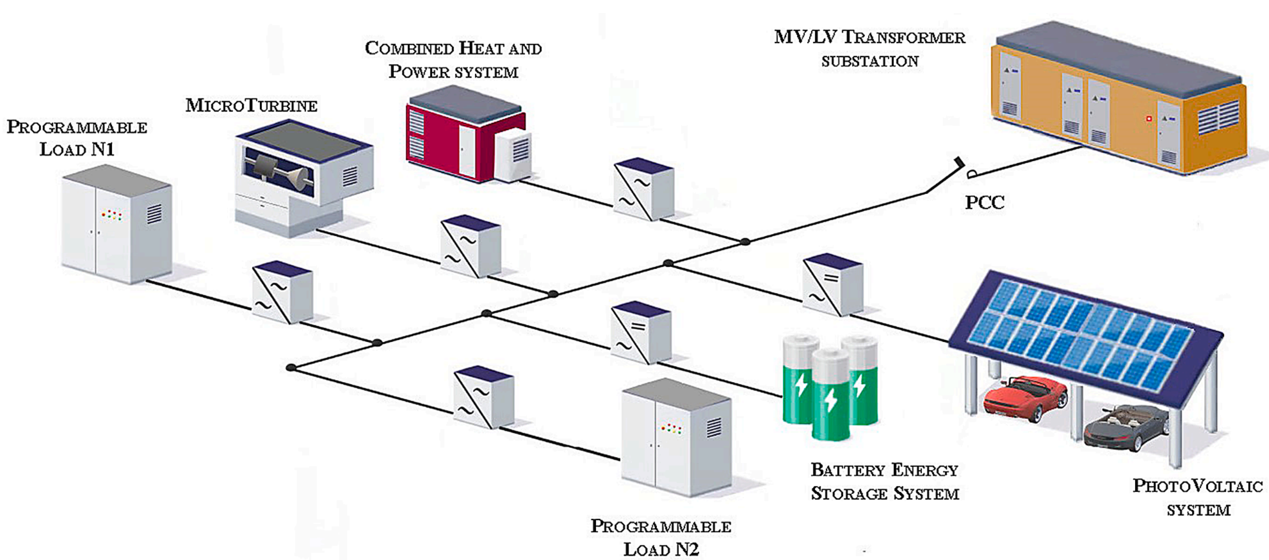

Fig. 2. The schematic single-line diagram of the PrInCE Lab experimental MG.

be sent to the local controllers of DGs inverters to be actualized. It is worth noting that the PID regulators are separately designed for each DGs considering their own dynamic models. The PID controllers' parameters can be tuned via *PID Tuner Function* of the Matlab–Simulink as suggested in [37].

3. Test results

The proposed control methodology has been tested on a subset of the energy sources available within the PrInCE Lab experimental MG built at the Polytechnic of Bari as shown in Fig. 2. Further details about this system and its components can be found in [38].

As shown in Fig. 2, the MG consists in a low-voltage radial distribution network which is connected to the main grid through a MV/LV transformer substation. This allows the MG to exchange power with the utility grid up to a maximum capacity of 250 kVA. The adopted configuration of the testbed MG includes dispatchable and non-dispatchable generation units along with an energy storage system. The DG units include a 30 kW MT and a 120 kW CHP, both powered by natural gas. The N-DRG units include a 50 kWp PV plant. Instead, the ESS consists of a 60 kW BESS. All these components provide power to two programmable loads, each with a rated power of 150 kVA. The technical and cost characteristics of both MT and CHP are reported in Table 1, whereas the technical characteristics of the BESS are shown in Table 2.

For simulation and testing purposes, the MG is implemented in the Matlab/Simulink environment [39] according to the block diagram shown in Fig. 3.

Three "*From Workspace*" blocks have been used as sources to import the real-time measurements of the active power absorbed by the load and provided by the PV plant, as well as the active power set-points of the BESS provided by the day-ahead economic dispatch methodology. Finally, in order to mimic the dynamic responses of the CHP, MT and BESS to set-point changes, a simplified time-invariant dynamic model for each of them has been *prior* derived. Details on these models are given in the following subsection.

3.1. Dynamic models of the CHP, MT and BESS

In order to simulate the dynamic behavior of the BESS, the simplified time-invariant dynamic model developed in [37] has been adopted.

The *Matlab System Identification Toolbox* has been instead used to identify both the CHP and the MT dynamic models. More in detail, the model identification process for the CHP system began by performing several experimental tests on this unit aimed at evaluating its dynamic response to different step changes of its active power setpoints. The data collected from these experiments are then passed to the Identification tool where they are processed to identify the transfer function that better approximates the behavior of the CHP plant. Following the same procedure also for the MT, with the information collected during the experimental tests and the *System Identification toolbox*, the transfer function better approximating the behavior of this plant has been obtained. The identified transfer functions for both CHP and MT are reported in Table 3.

Note that a one zero - three poles transfer function is adopted to accurately replicate the dynamic response of the CHP, whereas a one zero - two poles transfer function is adopted for the MT.

Table 1
The technical and cost characteristics of DGs.

Generator	Technical constraints		Cost coefficients [33]		
	P_{min} [kW]	P_{max} [kW]	α_{DG_i} [€/kW^{2}h]	β_{DG_i} [€/kWh]	γ_{DG_i} [€/h]
CHP	0	120	6.23×10^{-6}	0.0817	0.8010
MT	0	30	2.25×10^{-5}	0.0820	0.6483

Table 2
The technical characteristics of the BESS.

Storage device	Installed capacity	Storage capacity	Technical constraints			
			P_{min}	P_{max}	SOC_{min}	SOC_{max}
	[kW]	[kWh]	[kW]	[kW]	[%]	[%]
BESS	60	180	-60	+60	12	98

Once the CHP and MT models are identified, the PID regulators of both these sources were separately designed.

3.2. Simulation results

Based on the above test simulation setup, a comparative analysis was performed with another economic dispatching methodology in the two following scenarios to test the performances of the proposed methodology:

Scenario 1 – This test was performed on 24-hours to verify the ability of the proposed controller to optimize the online operation of the MG.

Scenario 2 – This test was aimed at investigating on the controller's ability to deal with the unavailability of one or more DGs to provide the regulation service.

For all computer simulations it was assumed that the MG operates as an energy price taker and cannot sell energy to the main grid.

Scenario 1

In this test, the performance of the proposed control methodology has been tested by simulating the real-time operation of the experimental MG over the 24-hour time window starting from midnight on October 28, 2023. To evaluate the improvements introduced by the developed control methodology, a comparison of performance was carried out with another economic dispatching methodology. To achieve this, a preliminary day-ahead operation planning of the MG was performed according to [40] by considering the 15-min day-ahead forecast profiles of PV production, total load demand, and the electricity market price shown in the Figs. 4,5. The main results of this analysis are reported in Figs. 6–8.

Note that under the above assumptions, MG was scheduled to purchase a significant amount of energy to satisfy its internal load demand when the day-ahead electricity market price was lower than the production costs of its internal energy sources (such as 12:00 – 15:00). Conversely, when the day-ahead electricity market price is high, the MG was scheduled to fulfill the internal load demand with energy locally produced, avoiding thus to exchange power with the utility grid. More in detail, it can be observed that the CHP, due to its lower production costs, was scheduled to provide the greatest contribution to satisfying the internal load demand. On the contrary, the BESS's contribution to the internal load satisfaction is limited by the need to extend their usage over the whole day.

Starting from the day-ahead economic dispatch results, the MG's online operation was simulated by using the hourly electricity price on the intraday market, along with daily load and PV power profile recorded with a sample time of 1 second. Figs. 9,10 show the time-domain behavior of these input data.

The resulting time-domain behavior of the tie-line active power flow is shown in Fig. 11.

Note that during the overnight period, specifically between 00:00 and 06:00, as the actual load demand is lower than the forecasted one, the MG is forced to give the surplus of energy generated by its internal energy resources to the main grid. Since the MG is not authorized to sell energy to the main grid, it was not paid for supplying this energy, resulting in economic loss. Conversely, for all other hours of the day, forecast errors in load and PV production forced the MG to purchase more energy from the utility grid than the scheduled one to fulfill the internal load demand, resulting in higher energy costs.

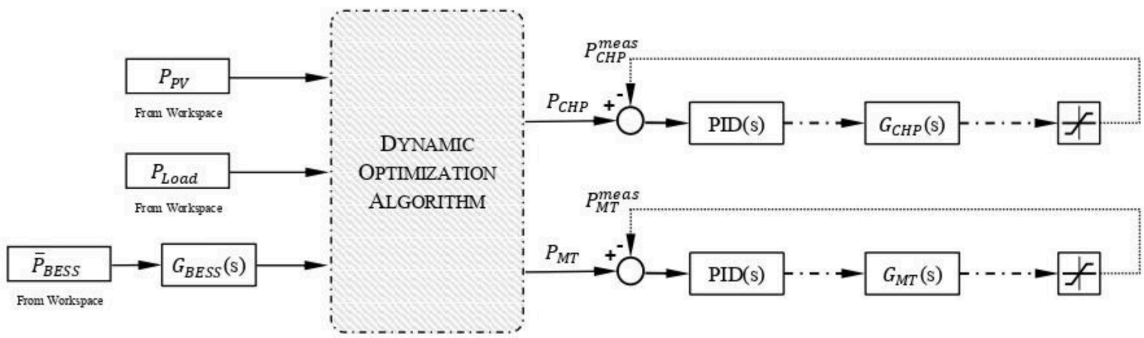

Fig. 3. Simplified model of the PrInCE Lab experimental MG.

Table 3
Identified transfer function of simplified models of CHP and MT.

Generator	Transfer function
CHP	$G_{CHP}(s) = \dfrac{2123\,s + 254.5}{s^3 + 10550\,s^2 + 2400\,s + 268.8}$
MT	$G_{MT}(s) = \dfrac{-2.92\,s + 1.33}{s^2 + 11.79\,s + 1.36}$

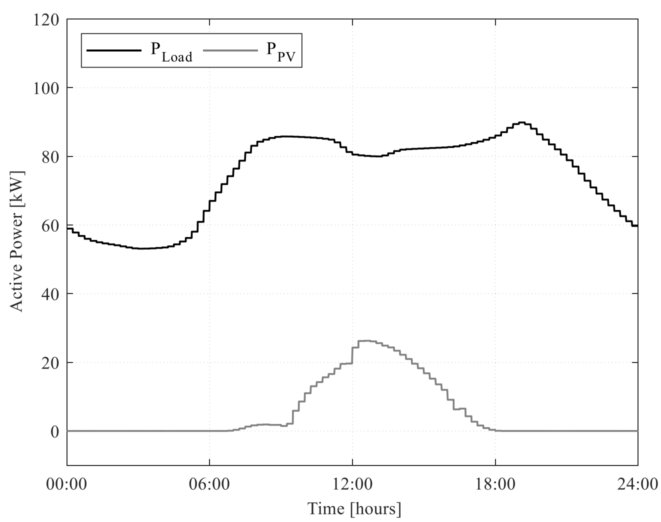

Fig. 4. The forecast curve of the PV and load demand for the 15 min period.

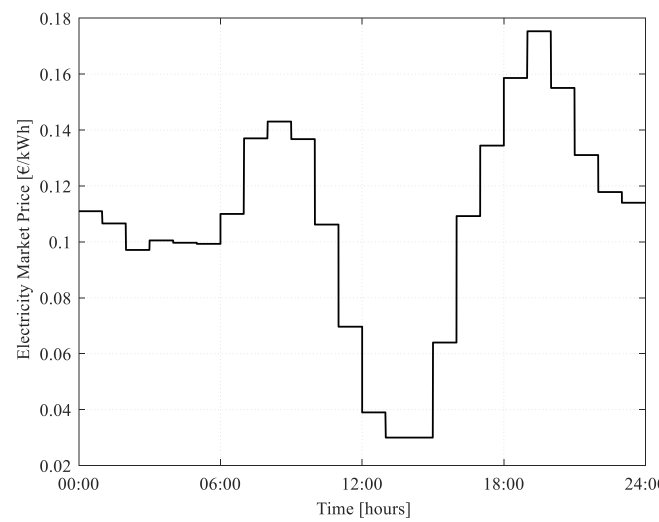

Fig. 5. The forecast curve of the electricity market price for the 15 min period.

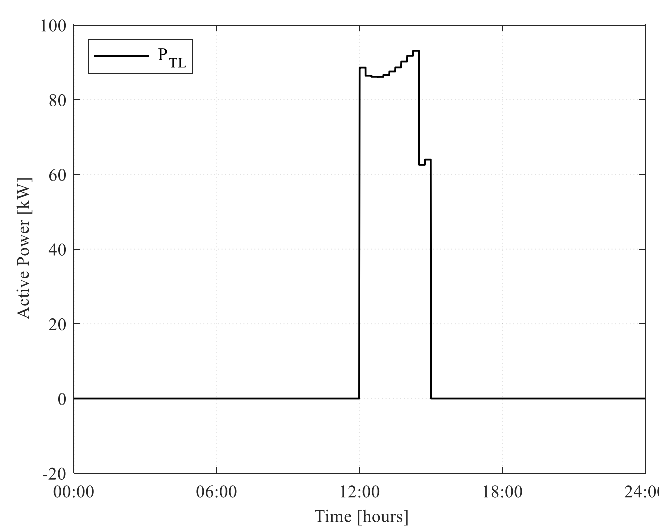

Fig. 6. The 15-minutes P_{TL} day-ahead schedule.

To assess the enhancements that can be obtained by applying the proposed methodology, it was tested under the same real-time operating conditions and assuming that the BESS was managed in accordance with its day-ahead economic dispatch schedule. The obtained results are reported in Figs. 12,13. More in detail, Fig. 12 shows the time domain behavior of the resulting tie-line active power flow, whereas in Fig. 13 the obtained time domain behaviors of both CHP and MT are reported.

As can be noted, the proposed methodology has efficiently managed the active power outputs of both CHP and MT allowing the MG to adapt its internal production to the actual load demand and to the intraday electricity market price. More in detail, to avoid giving energy to the main grid without being paid, the proposed methodology forced the tie-line active power flow to be always close to zero, except for the period between 13:00 and 15:00, when the methodology revealed that it is more convenient to purchase energy from the grid than to produce it internally. This is mainly because the electricity market prices were lower than the production costs of DGs owned by the MG.

An economic analysis was carried out to assess the effectiveness of the proposed methodology based on the results obtained from the real-time operation of the MG with and without controller. The obtained results are reported in Table 4.

Note that the proposed online control methodology was able to reduce the total operating costs of the MG from a value of 178.58 €/day in the non-optimized condition to the value of 169.58 €/day resulting in an improvement of 5 %.

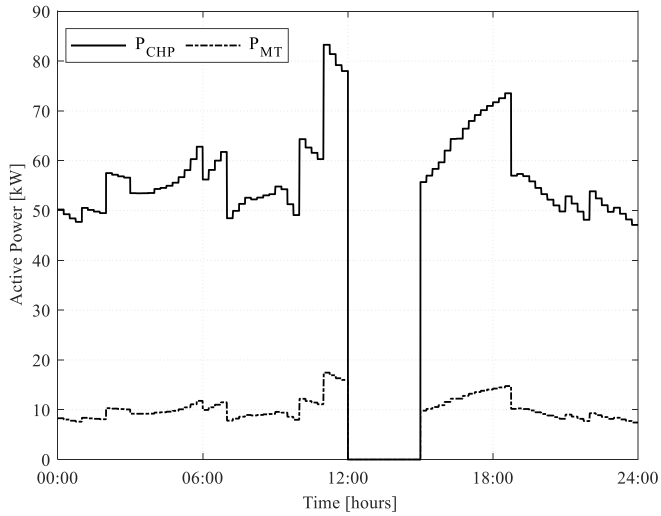

Fig. 7. The day-ahead operation plan over 15-minutes time horizon of both P_{CHP} and P_{MT}.

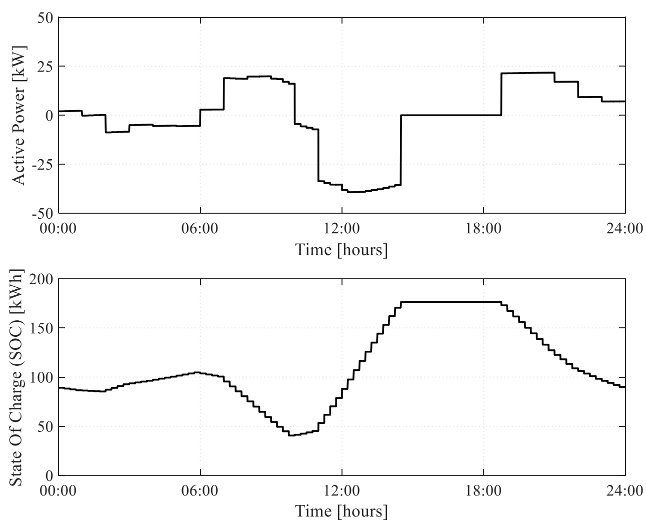

Fig. 8. The day-ahead operation plan of the BESS.

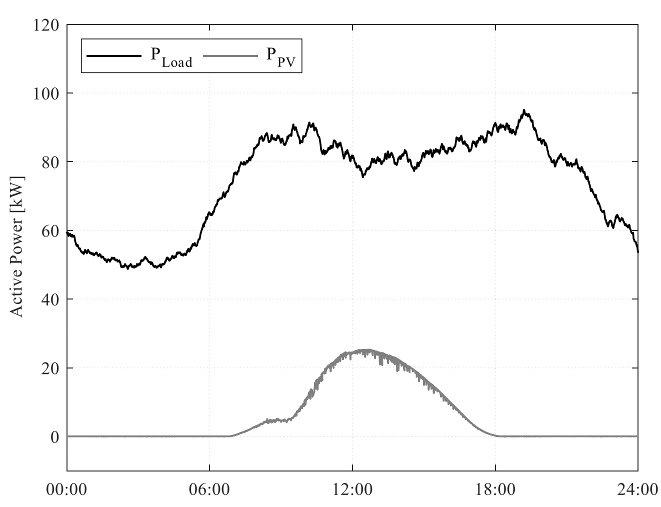

Fig. 9. Daily profiles of load demand and PV.

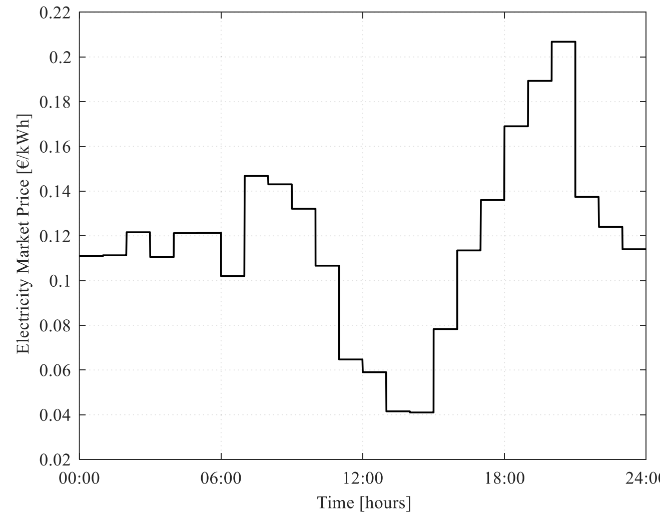

Fig. 10. The hourly intraday electricity market price.

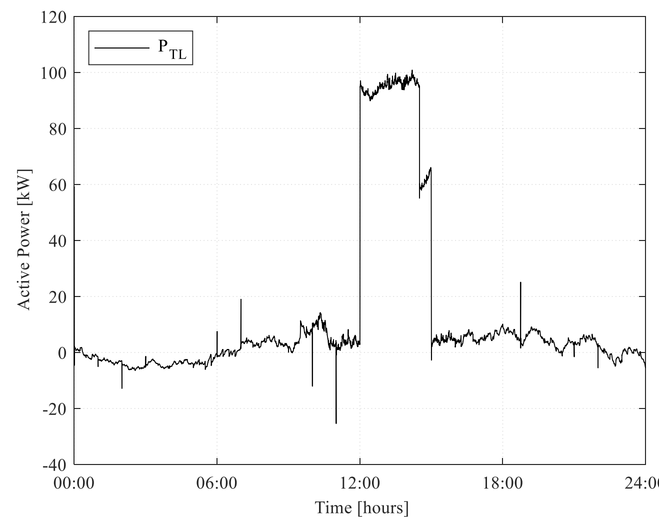

Fig. 11. Time domain behavior of the tie-line active power flow.

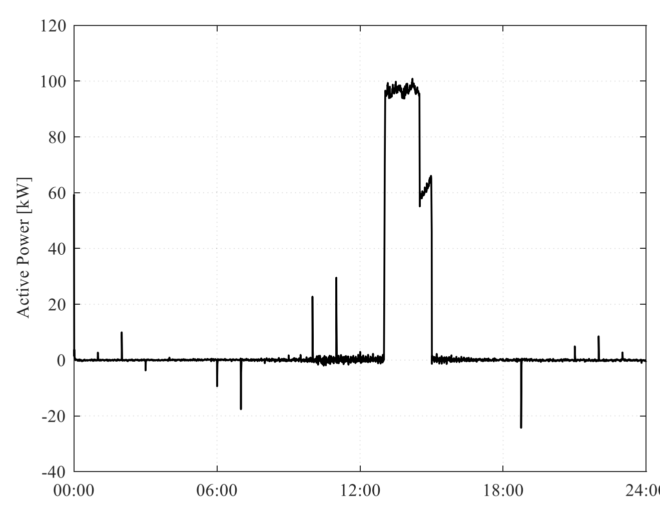

Fig. 12. Time domain behavior of the tie-line active power flow.

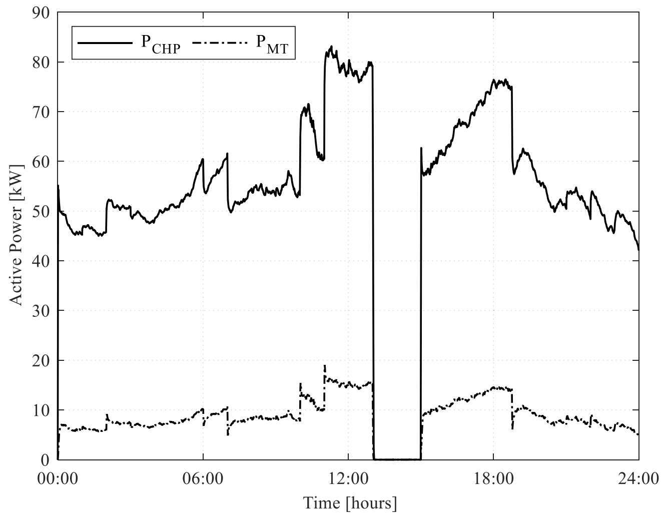

Fig. 13. Time domain behavior of the CHP and MT active power outputs.

Table 4
MG's costs with and without the controller.

MG Costs [€/day]	**Real-time operation**	
	Without online controller	**With online controller**
Costs of purchasing energy from the grid	33.30	13.89
Costs of generation from CHP	112.46	123.62
Costs of generation from MT	32.82	32.38
Total MG costs	**178.58**	**169.58**

Scenario 2

In order to investigate the self-adaptability of the proposed controller, another test was performed under the same operating conditions adopted in the previous test case by simulating the following sequential scenarios reported in Table 5.

In Figs. 14–16 are shown, respectively, the time domain behaviors of the PV and BESS as well as the obtained control laws for the tie-line active power flow, CHP and MT active power outputs.

As a result of the PV trip at $t = 12{:}00$ a rapid rising of the tie-line active power flow occurred with a consequent increase in the MG operating costs. In an effort to minimize them, the proposed methodology suddenly reacted by regulating the active power injections of CHP and MT. More specifically, it can be seen that in the time period between 12:00 to 13:00 both CHP and MT have been called to increase their active power outputs depending on their own contribution to the objective function. Taking advantage of the lower intraday electricity market prices, the controller forces the MG to purchase all the energy required to satisfy the internal load demand from the main grid, keeping the active power injections of the CHP and MT at zero. Because of the BESS outage at $t = 16{:}00$, the controller promptly reacted sharing the resulted active power imbalance among the CHP and MT so as not to involve the main grid in the regulation service. Therefore, the tie-line active power flow is kept around to zero as shown in Fig. 15. The unexpected MT failure at $t = 22{:}00$ resulted in an active power imbalance

Table 5
Time list of failure events.

Operating scenarios	**Time** [hours]
PV generation trip	12:00
BESS outage	16:00
MT failure	22:00

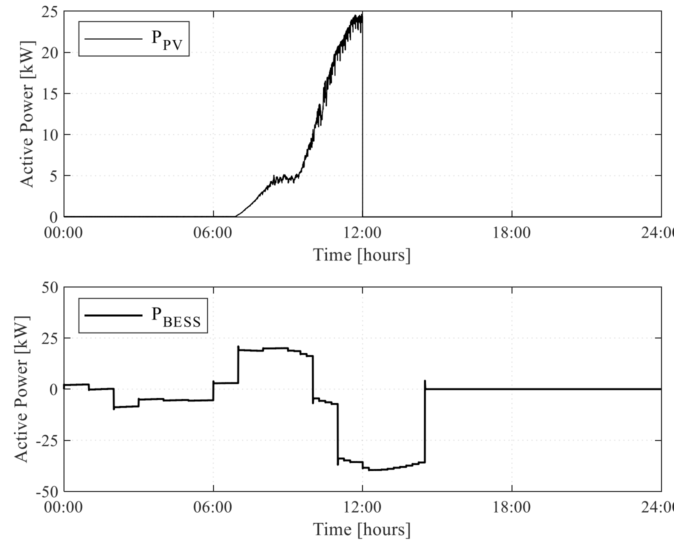

Fig. 14. Time domain behavior of PV and BESS active power outputs when a failure occurs.

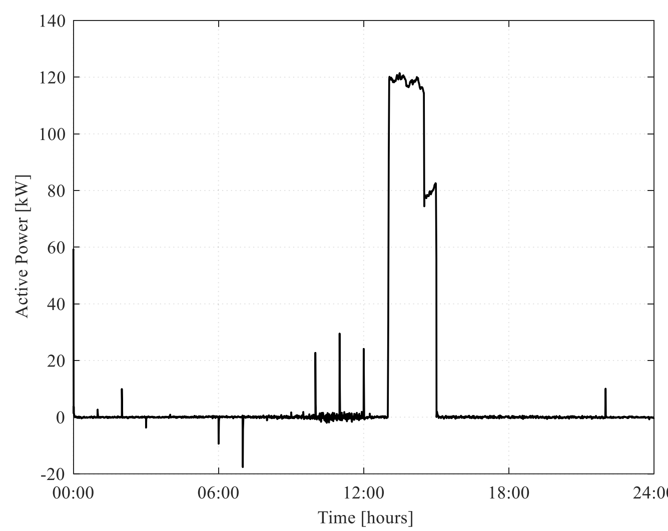

Fig. 15. Time domain behavior of the tie-line active power.

that the controller promptly detected. To prevent paying excessive prices for grid energy, the controller forced the CHP to raise active power output to balance the overall internal load demand.

In order to investigate on the advantages brought by the proposed online control methodology, another simulation test was performed under the same operating conditions by assuming that the MG is managed on the basis of the day-ahead economic dispatch. The resulting tie-line active power flow has been shown in Fig. 17.

As can be seen, in this case due to the absence of the control action, all power imbalances that occur within the MG following the unavailability of one or more energy resources are promptly compensated by the main grid. As result the MG moved into a suboptimal operating condition.

Based on the results obtained with and without controller, an economic analysis was performed. The main results are summarized in Table 6.

As can be noted, in this scenario thanks to the ability of the proposed controller to suddenly react to the unavailability of one or more energy resources it was possible to adjust in the continuous time domain the active power outputs of all DGs involved in the regulation service. As

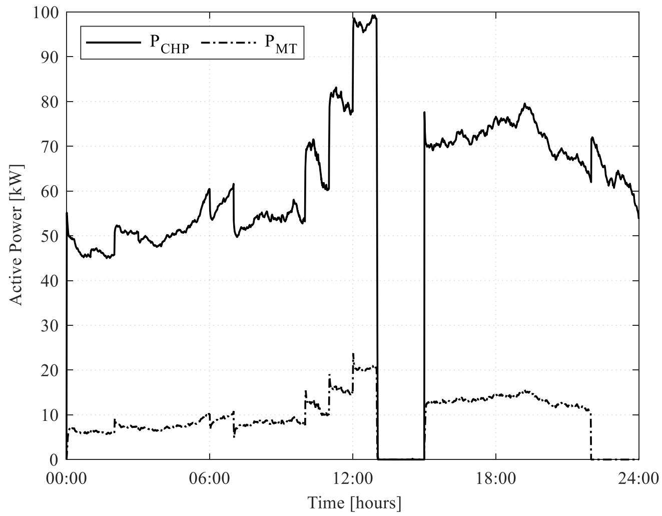

Fig. 16. Time domain behavior of CHP and MT active power outputs.

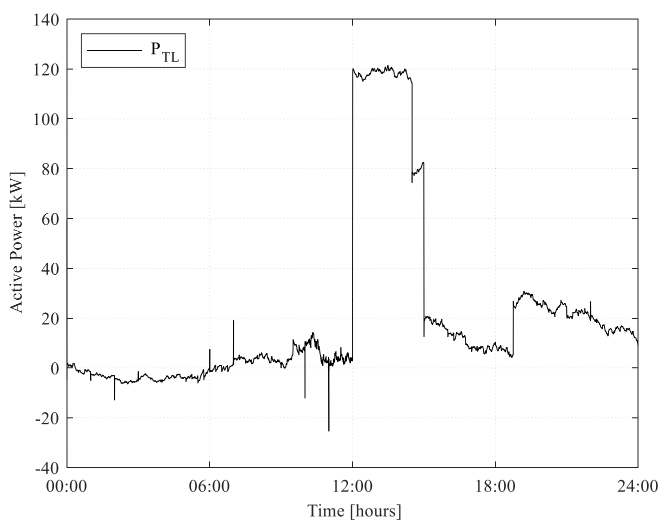

Fig. 17. Time domain behavior of the tie-line active power flow.

Table 6
MG's costs with and without the controller.

MG Costs [€/DAY]	**Real-time operation**	
	Without online controller	**With online controller**
Costs of purchasing energy from the grid	61.45	17.29
Costs of generation from CHP	112.46	133.47
Costs of generation from MT	31.47	33.33
Total MG costs	**205.40**	**184.09**

consequence the total MG operating costs are minimized from the value of 205.40 €/day in the non-optimized condition to the value of 184.58 €/day, resulting in an improvement of 10 %.

4. Conclusions

In this paper, a cooperative control methodology has been developed for the online energy management of the grid-connected MGs. The basic idea is to find the best compromise between the amount of energy produced internally by the MG and that exchanged with the upstream network so as to balance the internal load at the lowest operating costs. To comply with this requirement, a constrained dynamic multi-objective optimization problem has been formulated, considering three conflicting objective functions. An optimization algorithm based on the Lyapunov theorem embedding the sensitivity theory has been employed to find the optimal solution that simultaneously satisfies all these objectives at any instant of time.

In order to investigate on the performance of the proposed control methodology under different operating conditions, two computer simulations were carried out on the PrInCE Lab experimental MG. The obtained results demonstrated that the proposed controller regulates the sharing of active power load demand among MG's DGs and the main grid, based on their individual contribution to the objective function. Due to this feature, the proposed controller is able to avoid the generation of excessive active power from internal DGs and the absorption of unnecessary power from the main grid. Simulations also demonstrated the controller's ability to cope with the unavailability of one or more energy sources to provide the required amount of active power. In fact, in this case, the controller was able to automatically share the control burden previously assigned to the tripped sources among all the remaining DGs, moving the MG in a suboptimal operating condition. Furthermore, the economic analysis revealed that the proposed methodology results in savings of approximately 5 % compared to the non-optimized condition. These economic benefits become even more evident when an unexpected failure of one or more components within the MG occurs. In fact, in this case the proposed controller saves about 10 % compared to the scenario where no control action was applied to the MG.

CRediT authorship contribution statement

A. Cagnano: Writing – review & editing, Writing – original draft, Validation, Software, Methodology. **E. De Tuglie:** Writing – review & editing, Supervision, Methodology, Conceptualization. **A. Introna:** Writing – original draft, Visualization, Software, Methodology, Formal analysis, Data curation. **P. Montegiglio:** Software, Methodology. **A. Passarelli:** Software, Methodology.

Declaration of competing interest

The authors declare the following financial interests/personal relationships which may be considered as potential competing interests:

Enrico De Tuglie reports financial support was provided by European Union. If there are other authors, they declare that they have no known competing financial interests or personal relationships that could have appeared to influence the work reported in this paper.

Data availability

Data will be made available on request.

Acknowledgments

European Union Next-GenerationEU (National Recovery and Resilience Plan (NRRP), Mission 4 Component 2 Investment 1.3) under the Network 4 Energy Sustainable Transition (NEST) Extended Partnership (Italian Ministry of University and Research Decree No. 1561 of 11/10/2022) under Project PE00000021.

References

[1] T.D. De Lima, J.F. Franco, F. Lezama, J. Soares, A specialized long-term distribution system expansion planning method with the integration of distributed energy resources, IEEe Access. 10 (2022) 19133–19148, https://doi.org/10.1109/ACCESS.2022.3146799.

[2] T.T. Mai, P.H. Nguyen, Q.T. Tran, A. Cagnano, G. De Carne, Y. Amirat, A.T. Le, E. De Tuglie, An overview of grid-edge control with the digital transformation, Electr. Eng. 103 (2021) 1989–2007, https://doi.org/10.1007/s00202-020-01209-x.
[3] N. Daryani, K. Zare, S. Tohidi, Design for independent and self-adequate microgrids in distribution systems considering optimal allocation of DG units, IET Gen. Transm. Distrib. 14 (2020) 728–734, https://doi.org/10.1049/iet-gtd.2019.0379.
[4] A. Cagnano, De Tuglie E, M. Dicorato, G. Forte, M. Trovato, PV plants for voltage regulation in distribution networks, in: 2012 47th International Universities Power Engineering Conference (UPEC), Uxbridge, UK, 2012, pp. 1–5, https://doi.org/10.1109/UPEC.2012.6398422.
[5] A. Akimov, J. Inchauspe, M. Mouritz, A. Silva, Are Australian regulatory and policy frameworks ready for a distributed-energy-resources-led energy transition? Austr. J. Public Admin. 82 (2023) 529–556, https://doi.org/10.1111/1467-8500.12609.
[6] M. Khorasany, M. Raoofat, Bidding strategy for participation of virtual power plant in energy market considering uncertainty of generation and market price, in: 2017 Smart Grid Conference (SGC), Tehran, Iran, 2017, pp. 1–6, https://doi.org/10.1109/SGC.2017.8308846.
[7] P.L. Querini, O. Chiotti E. Fernádez, Cooperative energy management system for networked microgrids, Sustain. Energy Grids Netw. 23 (2020), https://doi.org/10.1016/j.segan.2020.100371.
[8] A. Cagnano, E. De Tuglie, P. Mancarella, Microgrids: overview and guidelines for practical implementations and operation, Appl. Energy 258 (2020), https://doi.org/10.1016/j.apenergy.2019.114039.
[9] A. Mohammed, H. Abu-Rub, A Co-Simulation Platform for Microgrid Integration into Transmission System - Power Quality Study, in: 2022 10th International Conference on Smart Grid (icSmartGrid), Istanbul, Turkey, IEEE, 2022, pp. 319–324, https://doi.org/10.1109/icSmartGrid55722.2022.9848679.
[10] R.H. Lasseter, Microgrids and distributed generation, J. Energy Eng. 133 (2007) 144–149, https://doi.org/10.1061/(ASCE)0733-940.
[11] M.K. Karugarama, Mitigation of Blackout in Kigali Using a Microgrid with Advanced Energy Storage and Solar Photovoltaics, Doctoral dissertation, Virginia Tech, 2016.
[12] C.X. Dou, X.B. Jia, H. Li M. F. Lv, Multi-agent system based energy management of microgrid on day-ahead market transaction, Electr. Power Compon. Syst. 44.12 (2016) 1330–1344, https://doi.org/10.1080/15325008.2016.1158216.
[13] M. Zachar P. Daoutidis, Microgrid/macrogrid energy exchange: a novel market structure and stochastic scheduling, IEEE Trans. Smart Grid 8.1 (2017) 178–189, https://doi.org/10.1109/TSG.2016.2600487.
[14] J. Jimeno, J. Anduaga, J. Oyarzabal, A.G. de Muro, Architecture of a microgrid energy management system, Eur. Trans. Electr. Power 21.2 (2011) 1142–1158, https://doi.org/10.1002/etep.443.
[15] M.J. Vasallo, J.M. Bravo, A MPC approach for optimal generation scheduling in CSP plants, Appl. Energy 165 (2016) 357–370, https://doi.org/10.1016/j.apenergy.2015.12.092.
[16] R.S. Kumar, L.P. Raghav, D.K. Raju, A.R. Singh, Impact of multiple demand side management programs on the optimal operation of grid-connected microgrids, Appl. Energy 301 (2021), https://doi.org/10.1016/j.apenergy.2021.117466.
[17] R. Zhang, G. Li, S. Bu, S. Aziz R. Qureshi, Data-driven cooperative trading framework for a risk-constrained wind integrated power system considering market uncertainties, Int. J. Electr. Power Energy Syst. 144 (2023), https://doi.org/10.1016/j.ijepes.2022.108566.
[18] S. Talari, M. Yazdaninejad, M.R. Haghifam, Stochastic-based scheduling of the microgrid operation including wind turbines, photovoltaic cells, energy storages and responsive loads, IET Gen. Transm. Distrib. 9.12 (2015) 1498–1509, https://doi.org/10.1049/iet-gtd.2014.00400.
[19] I.N. Trivedi, D.K. Thesiya, A. Esmat, P. Jangir, A multiple environment dispatch problem solution using ant colony optimization for micro-grids, in: 2015 International Conference on Power and Advanced Control Engineering (ICPACE), Bengaluru, India, 2015, pp. 109–115, https://doi.org/10.1109/ICPACE.2015.7274927.
[20] S.X. Chen, H.B. Gooi, Q.M. Wang, Sizing of energy storage for microgrids, IEEE Trans. Smart Grid 3. 1 (2012) 142–151, https://doi.org/10.1109/TSG.2011.2160745.
[21] H. Khorramdel, J. Aghaei, B. Khorramdel P. Siano, Optimal battery sizing in microgrids using probabilistic unit commitment, IEEe Trans. Industr. Inform. 12.2 (2016) 834–843, https://doi.org/10.1109/TII.2015.2509424.
[22] D. Kumar, S. Dhundhara, Y.P. Verma, R. Khanna, Impact of optimal sized pump storage unit on microgrid operating cost and bidding in electricity market, J. Energy Storage 51 (2022), https://doi.org/10.1016/j.est.2022.104373.
[23] A.C. Luna, L.N. Diaz, F. Andrade, M. Graells, J.M. Guerrero, J.C. Vasquez, Economic power dispatch of distributed generators in a grid-connected microgrid, in: 2015 9th International Conference on Power Electronics and ECCE Asia (ICPE-ECCE Asia), Seoul, Korea (South), 2015, pp. 1161–1168, https://doi.org/10.1109/ICPE.2015.7167927.
[24] Z. Li, Y. Xu, Optimal coordinated energy dispatch of a multi-energy microgrid in grid-connected and islanded modes, Appl. Energy 210 (2018) 974–986, https://doi.org/10.1016/j.apenergy.2017.08.197.
[25] W. Mao, N. Dai, H. Li, Economic dispatch of microgrid considering fuzzy control based storage battery charging and discharging, J. Electr. Syst. 15.3 (2019) 417–428. https://search.emarefa.net/detail/BIM-892753.
[26] H. Farzin, M. Fotuhi-Firuzabad, M. Moeini-Aghtaie, A stochastic multi-objective framework for optimal scheduling of energy storage systems in microgrids, IEEE Trans. Smart Grid 8.1 (2017) 117–127, https://doi.org/10.1109/TSG.2016.2598678.
[27] M. Nikzad, A. Samimi, Integration of designing price-based demand response models into a stochastic bi-level scheduling of multiple energy carrier microgrids considering energy storage systems, Appl. Energy. 282 Part A (2021), https://doi.org/10.1016/j.apenergy.2020.116163.
[28] E. Rahmani, S. Mohammadi, M. Zadehbagheri, M. Kiani, Probabilistic reliability management of energy storage systems in connected/islanding microgrids with renewable energy, Electr. Power Syst. Res. 214 (2023), https://doi.org/10.1016/j.epsr.2022.108891.
[29] M. Premkumar, R. Sowmya, C. Ramakrishnan, P. Jangir, E.H. Houssein, S. Deb, N. M. Kumar, An efficient and reliable scheduling algorithm for unit commitment scheme in microgrid systems using enhanced mixed integer particle swarm optimizer considering uncertainties, Energy Rep. 9 (2023) 1029–1053, https://doi.org/10.1016/j.egyr.2022.12.024.
[30] D. Rasolomampionona, E. De Tuglie, A. Cagnano, F. Marcone, G. Porro, Economic dispatch for on-line operation of grid-connected microgrids, bulletin of the Polish academy of sciences, Techn. Sci. 68.4 (2020), https://doi.org/10.24425/bpasts.2020.134179.
[31] S. Zeinal-Kheiri, A. Mohammadpour Shotorbani, A. Khardenavis, B. Mohammadi-Ivatloo, R. Sadiq, K. Hewage, An adaptive real-time energy management system for a renewable energy-based microgrid, IET Renew. Power Gen. 15 (13) (2021) 2918–2930, https://doi.org/10.1049/rpg2.12223.
[32] F. Jiao, C. Ji, Y. Zou X. Zhang, Tri-stage optimal dispatch for a microgrid in the presence of uncertainties introduced by EVs and PV, Appl. Energy 304 (2021), https://doi.org/10.1016/j.apenergy.2021.117881.
[33] A.M. Shotorbani, S. Zeinal-Kheiri, G. Chhipi-Shrestha, B. Mohammadi-Ivatloo, R. Sadiq, K. Hewage, Enhanced real-time scheduling algorithm for energy management in a renewable-integrated microgrid, Appl. Energy 304 (2021), https://doi.org/10.1016/j.apenergy.2021.117658.
[34] A. Cagnano, E. De Tuglie, P. Gibilisco, Assessment and control of microgrid impacts on distribution networks by using experimental tests, IEEE Trans. Ind. Appl. 55 (6) (2019) 7157–7164, https://doi.org/10.1109/TIA.2019.2940174.
[35] W. Shi, N. Li, C.-C. Chu, R. Gadh, Real-time energy management in microgrids, IEEE Trans. Smart Grid. 8 (1) (2017) 228–238, https://doi.org/10.1109/TSG.2015.2462294.
[36] A. Cagnano, A. Caldarulo Bugliari, E. De Tuglie, A cooperative control for the reserve management of isolated microgrids, Appl. Energy 218 (2018) 256–265, https://doi.org/10.1016/j.apenergy.2018.02.142.
[37] E. De Tuglie, G. Graditi, A. Introna, P. Montegiglio, A. Passarelli, Minimization of microgrid impact on distribution network systems through BESS real-time control, in: 2022 Workshop on Blockchain for Renewables Integration (BLORIN), Palermo, Italy, 2022, pp. 91–96, https://doi.org/10.1109/BLORIN54731.2022.10028348.
[38] A. Cagnano, E. De Tuglie, L. Cicognani, Prince—electrical energy systems lab: a pilot project for smart microgrids, Electr. Power Syst. Res. 148 (2017) 10–17, https://doi.org/10.1016/j.epsr.2017.03.011.
[39] Matlab/Simulink User's Guide, The math works.
[40] P. Gibilisco, G. Ieva, F. Marcone, G. Porro, E. De Tuglie, Day-ahead operation planning for microgrids embedding battery energy storage systems. A case study on the PrInCE Lab microgrid, in: 2018 AEIT International Annual Conference, Bari, Italy, 2018, pp. 1–6, https://doi.org/10.23919/AEIT.2018.8577353.